Indoor Localization in Current 5G Networks: The Way to Go

Antonin Le Floch
Alsatis, Université de Toulouse, CNRS,
Toulouse INP, UT3
Toulouse, France
antonin.lefloch@irit.fr

Rahim Kacimi
Université de Toulouse, CNRS,
Toulouse INP, UT3
Toulouse, France
rahim.kacimi@irit.fr

Pierre Druart
Alsatis
Toulouse, France
pierre.druart@alsatis.com

Yoann Lefebvre
Alsatis
Toulouse, France
yoann.lefebvre@alsatis.com

André-Luc Beylot
Université de Toulouse, CNRS,
Toulouse INP, UT3
Toulouse, France
andre-luc.beylot@irit.fr

***Abstract*—Localization in 5G networks perfectly illustrates how cellular networks strive to handle all wireless use cases. However, despite the growing interest around indoor localization, the complex radio environment along with the lack of standard-compliant equipment make positioning in 5G networks a daunting task. Although some previous works have proposed experimental solutions, none has ever tackled a comprehensive scheme based on real-life 5G networks. Therefore, the purpose of our paper is to address the most exhaustive solution, taking advantage of all the possibilities offered today by the 5G ecosystem. This new vision emphasizes efficiency, practicality, and offers current 5G networks a localization service with a precision of around 3 meters. To do so, an analysis of all possible localization methods is conducted, retaining only those deemed satisfactory, namely fingerprinting and Pedestrian Dead Reckoning (PDR). Subsequently, we combine these two solutions, where the shortcomings of one are compensated by the strengths of the other. Through extensive experiments, we demonstrate that our PRILUN fusion algorithm outperforms fingerprinting, PDR, and other similar approaches. Extensive real-life experiments in our 5G infrastructure highlight the performance expected to date in a typical 5G network. This paper therefore paves the way for the most comprehensive indoor localization solution in current 5G networks.**

***Index Terms*—5G, Indoor Localization, Fingerprinting, Pedestrian Dead Reckoning, Experimentation, Fusion**

I. Introduction

The synergy between localization and 5G represents a significant advantage for innovative networks aiming for digital frugality. Our aim here is to accurately locate at-risk workers at Toulouse Hospital by leveraging the existing 5G private network. In this article, we present how a new comprehensive solution is first developed and tested inside the Alsatis [1] 5G private network before deployment in May 2024.

Although localization is firmly anchored by the 3rd Generation Partnership Project (3GPP) in 5G Release 16, the proposed functions and protocols are still not supported by most commercial equipment. Furthermore, localization inside buildings remains a major challenge, given the extremely difficult environment of multipath and non-line-of-sight (NLOS). This is further exacerbated by networks primarily designed for data transmission, and therefore the maximization of coverage area to the detriment of overlapping zones essential for localization. While some experimental studies have been conducted [2]–[6], none consider a scheme using all possibilities offered by current commercial off-the-shelf (COTS) equipment in 5G networks.

Here, we argue for a comprehensive, large-scale, universal, and practical approach that takes advantage of the existing 5G networks. Such a solution should leverage all possible tools given by 5G while being easily deployed today in any network. As our aim is to provide the most advanced solution to date, we must first determine the localization paradigm to be used. Among the plethora of localization methods to consider, four main families have been identified: temporal, angular, fingerprinting, and dead reckoning. In the following, we will analyze them to assess their suitability for localization in current 5G networks.

Temporal methods often operate by measuring the time difference between synchronous signals, as illustrated in Figure 1. Both downlink using Positioning Reference Signal (PRS) and uplink using Sounding Reference Signals (SRS) can be employed. The latter is currently used by the Geo 5G project [5] and promises performance down to 1 m. However, there is currently no COTS equipment capable of analyzing PRS or SRS signals. Moreover, these systems require a direct line-of-sight (LOS), minimal multipath interference, and reception from at least three cells to apply trilateration algorithms. Achieving these conditions is far from common in a data-oriented network, as depicted by our realistic 5G deployment in Figure 3. A 5G network suitable for SRS requires three to four times as many Next Generation NodeB (gNB), multiplying CAPEX by the same amount. Although temporal methods are promising and offer a glimpse into the future of localization in ultra dense networks, they cannot yet be used.

ISBN 978-3-903176-63-8 © 2024 IFIP

Angular methods are based on antenna-level measurements and take advantage of downlink beamforming or uplink phase difference, as shown in Figure 2. Retrieving the angle requires deep physical signal analysis, today only possible with substantial developments on Software Defined Radio (SDR). Moreover, measuring the angle proves to be inherently imprecise, as highlighted by articles that address the topic [6]. Furthermore, this method is only suitable for use close to the antenna, as the greater the distance from the target, the greater the impact of angular error. Finally, there is currently no COTS Massive MIMO or beamforming equipment suitable for indoor use. There is still much to be done to benefit from the angular method, with current research positioning it as a complementary solution to existing methods.

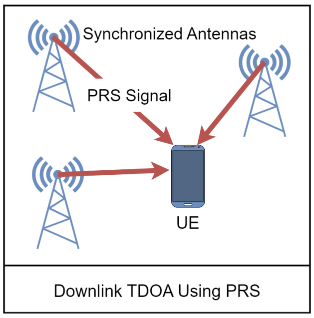

Fig. 1. Time Difference of Arrival using PRS.

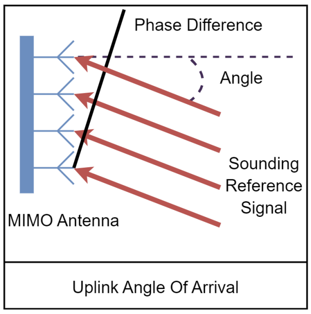

Fig. 2. Angle of Arrival using phase difference.

Enhanced Cell Id (E-CID) methods encompass a range of localization techniques using the cell identifier and simple measurements of the physical signal, such as the Reference Signal Received Power (RSRP). The latter can be employed to implement a method known as fingerprinting, which involves comparing signal strength with a reference map. Proven effective in Wi-Fi [7], fingerprinting has been successfully implemented in some LTE [2] and 5G networks [8] composed of commercial equipment. This approach has already been addressed in our previous publication [4], with a comprehensive solution on how to effectively implement E-CID in a realistic 5G network. Our previous experiments offered an accuracy of the order of $1\,\mathrm{m}$ to $3\,\mathrm{m}$. The conclusion drawn position the combination of 3GPP E-CID and fingerprinting as an approach to be favored for localization in 5G.

Given the ubiquity of Inertial Measurement Units (IMUs) in smartphones, which can be leveraged for Pedestrian Dead Reckoning (PDR) navigation, we assert the importance of considering them to enhance localization in 5G. Having been employed since antiquity for navigation, dead reckoning involves utilizing distance and direction measurements to infer the current position from a known starting point. This method has demonstrated excellent results [9]–[13] and can operate independently or jointly with other localization solutions. It is therefore perfectly aligned with current 5G networks, as it requires neither dedicated topology nor specific hardware.

To conclude our analysis, fingerprinting or PDR do not require non-commercial equipment and a dedicated topology, unlike temporal and angular methods. These solutions are therefore the only two viable in a current 5G network. The next step is to assess these two methods, but before doing so, we will present the context of localization in a 5G network in Section II. This section also details the realistic 5G infrastructure deployed in Alsatis. We then evaluate fingerprinting in Section III and PDR in Section IV. The conclusions drawn allow us to design a fusion algorithm where the shortcomings of one are compensated by the strengths of the other. The latter is detailed and experimentally proven to outperform fingerprinting, PDR and similar algorithms in Section V. Section VI presents the state of the art, and Section VII concludes the paper.

II. Overview of Localization in a 5G Network

The importance of localization for the 3GPP is clearly reflected in the standards providing two protocols and two functions specifically dedicated to localization. These new features, illustrated in Figures 4 and 5, enable seamless localization of all end devices in any compliant network. Their definitions, purposes, and procedures are therefore detailed in the following. Finally, the commercial 5G infrastructure present in Alsatis is described in Section II-C.

A. *Localization Management Function*

In 5G, the User Equipment (UE) communicates with a gNB that constitutes the Radio Access Network (RAN). Both the UE and gNB can forward location-relevant data to the Location Management Function (LMF) [14] located in the Core Network (CN), as depicted in Figure 4. This function is responsible for both collecting all location-related information and executing an algorithm to estimate the position, making it a cornerstone of localization in 5G networks. This architecture allows centralized data collection while facilitating interoperability between UE, RAN, and CN. Furthermore, for security reasons, no telemetry can be transmitted to an external location function. The LMF is therefore mandatory to provide localization in 5G. A flaw in the specifications was identified, and thus an Advanced-LMF was proposed in a previous work [4]. By implementing this function in our CN, our framework can provide live position estimation of any device connected to the 5G network.

B. *Protocols*

To retrieve information, the LMF can rely on two protocols, as illustrated in Figure 4. The LTE Positioning Protocol (LPP) connects the UE to the LMF and is focused on retrieving all data measured by the end device along with side telemetry. Unfortunately, as far as we know, no commercial UE currently supports it. The LMF can also directly query the RAN via NR Positioning Protocol A (NRPPa). In doing so, the gNB requires measurements by the UE through Radio Resource Control (RRC) reconfigure messages. As RRC protocol is mandatory for any devices, this solution requires no specific developments on the UE side. NRPPa can thus be used to seamlessly retrieve the RSRP within the LMF and has been implemented accordingly in our infrastructure between an Amarisoft gNB [15] and the Halys 5G CN [16].

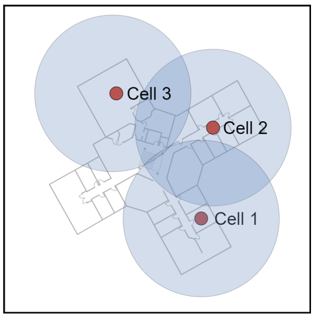

Fig. 3. Cell placement on first floor.

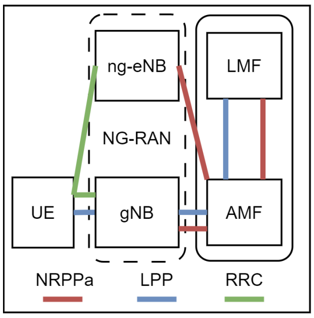

Fig. 4. 3GPP Localization specific protocols.

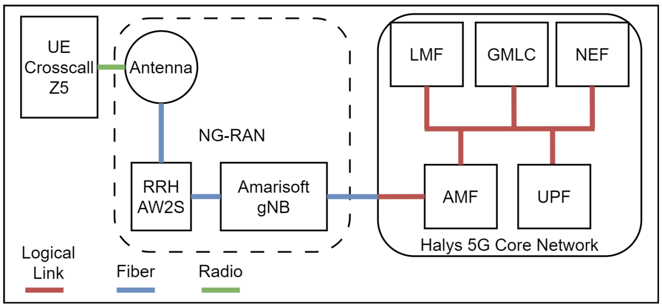

Fig. 5. Architecture of the 5G functions in our infrastructure.

C. A realistic 5G network

An infrastructure representative of a commercial 5G network was deployed throughout Alsatis. As illustrated in Figures 5 and 6, it includes a Halys 5G CN, an Amarisoft gNB, an AW2S Remote Radio Head (RRH) [17], and Crosscall 5G smartphones [18]. Several servers are dedicated to this setup, and antennas are distributed throughout the building, as shown in Figure 3 where three are on the first floor and two on the upper floor. Cell 1 operates with 4*4 Multiple Input Multiple Output (MIMO), while all others use 2*2 MIMO. The radios, along with an RRH and a Crosscall Z5 smartphone, are shown in Figure 6. The topology is oriented to maximize the coverage area, representing the way current 5G networks are designed. This concrete deployment thus perfectly reflects a typical private 5G network as deployed in a company, factory, shopping mall, or airport. All equipment used is off-the-shelf, enabling us to evaluate our solution using realistic hardware and software available worldwide.

Finally, some radio details are outlined in Table I and legal authorizations were given by French authority ARCEP in decision number 2022-1391, to transmit on the n77 band at 3.9–4.0 GHz.

TABLE I
RADIO PARAMETERS

Radio parameters on Amarisoft gNB			
Band	*ARFCN*	*Subcarrier Spacing*	*Bandwidth*
n77	663334	30 kHz	100 Mhz

Radio parameters were validated using radio tools.

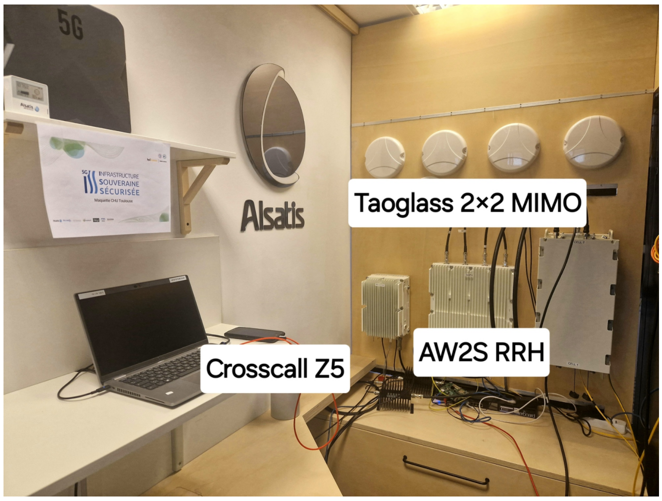

Fig. 6. COTS equipments used at Alsatis.

III. Fingerprinting with ECID: Insights, Innovations and Performance

As aforementioned in the introductory Section I, E-CID can be used to implement the proven fingerprinting approach in cellular networks. Some experiments on LTE or 5G infrastructure [2], [3] using Open Air Interface (OAI) and USRP b210 radios were proposed. None did consider the use of off-the-shelf equipment, nor a building-wide deployment, but rather a room-scale one. They also suggest custom schemes that are incompatible with 3GPP specifications. In this section, we highlight the key points of our previous work [4], which presents a concrete approach, taking advantage of current 5G network standards and features. Experiments are performed using our realistic 5G infrastructure at Alsatis to underline the expected performance of such a method.

A. Principle

In fingerprinting, the RSRP is compared with a reference map using a specialized Machine Learning (ML) algorithm. In the following, we discuss how the RSRP can be retrieved by the LMF, a reference map built, and models trained.

1) How to gather localization data with 3GPP function and protocols: Firstly, the RSRP must be collected within a location function, ideally in a seamless manner. This is accomplished in our infrastructure by using the NRPPa protocol and the LMF defined in Sections II-A and II-B. This major development is enabling multi RAN and CN compatibility. Moreover, as each positioning protocol and function is in the CN and only RRC protocol is used to retrieve data from the UE, it requires no applications or modifications on the UE side, making our system compatible with any 5G terminal.

2) A new approach in building a reference map: Secondly, an accurate RSRP reference map must be built to train the ML models. The preferred method in fingerprinting is to grid the building in one-meter increments. Although its simplicity and accuracy is not to question, the scalability of such a process poses a real challenge when designing a localization solution across all hospitals in a city. We therefore used an innovative method based on channel estimation and ray tracing and developed previously [4]. Its key benefits of scalability, ease of use and accuracy are confirmed through our experiments. This solution also differs from fingerprinting, requiring only a few measurements.

3) ML model: Finally, ML algorithms need to be defined and trained to predict the position from an RSRP measurement. This algorithmic aspect is detailed in the following Section III-B, as it provides a better understanding of how fingerprinting operates.

B. Algorithm and methodology insights

The purpose of these models is to estimate a position based on measured power and a reference map. This can be easily modeled by considering the set of measurements from m cells $RSRP = [rsrp_1, rsrp_2, \cdots, rsrp_m]$, reference points w_r, and a probability density $\delta_{i,r}$ of having power $rsrp_i$ from cell i at reference point w_r. Consequently, the most probable position of the user, denoted $\hat{w}$ can be deduced using equations (1) and (2).

$$P\left(RSRP \mid w_r\right) = \prod_{i=1}^{m} \delta_{i,r}(rsrp_i) \tag{1}$$

$$\hat{w} = \underset{1 \le r \le n}{arg\ max}\ P\left(RSRP \mid w_r\right) \tag{2}$$

Finding the most probable position is equivalent to identifying the reference points closest to our measurements. This corresponds to the k-Nearest Neighbors (k-NN) problem, prevalent in the fingerprinting literature [7]. As any ML algorithm, it is divided into Offline and Online phases.

1) Offline phase: During this phase, two models are trained using the reference map, as illustrated in the Figure 7. The first one is a classification model using the RSRP to predict the floor where the UE is located. The second one is a regression model that determines the precise position based on the measured RSRP and floor. This distinction stems from the discrete or continuous nature of the variables to be predicted.

The following is a very typical approach to model creation. The data from the reference map are first cleaned, normalized and divided into training, testing, and validation sets. Finally, models are defined and trained using the scikit-learn library [19]. We have carefully optimized these models, considering the number of neighbors, distance metric, and the execution time. After optimization, the models exhibit high accuracy, with $R^2 scores$ of 0.99 and 0.95 respectively. More details are provided in [4].

2) Online phase: During this phase, the RSRP is collected every $100\,\mathrm{ms}$, cleaned, and then the position is predicted. The cleaning phase may involve a sliding-window averaging system or a Kalman filter. Here, we considered a sliding window over a period of $10\,\mathrm{s}$. A Kalman filter was also tested, but no significant improvement was found. The averaged RSRP is then fed into the first model and the predicted floor is used as input for the second model.

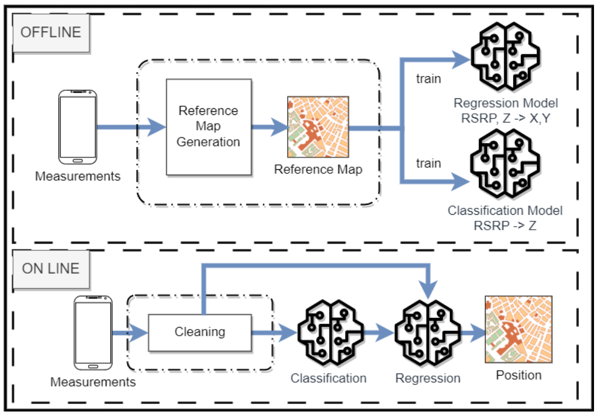

Fig. 7. Fingerprinting scheme.

C. Performance in a real 5G network

Using the infrastructure detailed in Section II-C, a measurement campaign was conducted throughout the building, achieving an average precision error of $3\,\mathrm{m}$. Three measurement points are isolated and presented in Figure 8 to underline the overall performance of our system. These points have been strategically chosen to represent the full range of situations encountered when using fingerprinting. On each, the signal was collected using a Crosscall Z5 smartphone connected to the 5G network. The error corresponding to each measurement point is illustrated in Figure 9.

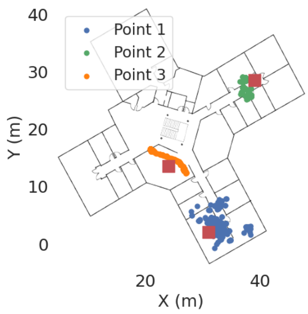

Fig. 8. Estimated position by ECID on three reference points.

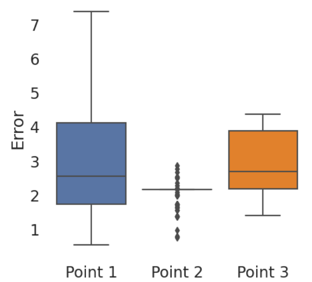

Fig. 9. Error on three reference points.

These three points represent typical cases of fingerprinting based localization. Point number 2, in direct line of sight and close to the antenna, exhibits almost constant and extremely low error. The other two points are situated in particularly challenging locations. Point 1 is isolated in one wing of the building and point 3 is located at the intersection of two zones, frequently performing handover between cells. Although the variance is substantial, the mean error is less than $3\,\mathrm{m}$, which perfectly meets the requirements of our use case while aligning with results reported in similar papers [2], [3], [7]. In-depth results are presented in [4] where LOS or human activity are studied.

IV. Pedestrian Dead Reckoning Navigation by Pedometer and Magnetometer: Description and Performance Analysis

IMUs are getting smaller, cheaper, more reliable and used in countless applications ranging from health measurements to car accident detection. Their ubiquity in 5G smartphone must therefore be considered when designing a localization scheme, as they also can be used for PDR. This ancient method, used since antiquity, consists in measuring a given distance denoted d_t and a direction denoted θ_t from a previous position initialized with (x_0, y_0) (3).

$$
\begin{aligned}
x_n &= x_0 + \sum_{t=1}^{n-1} d_t \cdot \cos(\theta_t) \\
y_n &= y_0 + \sum_{t=1}^{n-1} d_t \cdot \sin(\theta_t)
\end{aligned}
\tag{3}
$$

Seeking to model the movement of a pedestrian, the distance is a function of the number of steps and the step length, also known as the Step-and-Heading System (SHS). The direction is derived from the magnetometer, as elaborated in Section IV-B. This system relies heavily on proprietary IMUs and firmware, differing from phone to phone. Experiments are therefore conducted in Section IV-D to evaluate the performance and the overall coherence between phones. Many challenges remain to fully take advantages of PDR, and current research focuses on step detection, stride length prediction, and heading estimation [9]–[13].

A. Regarding the distance

Considering human movement, the distance d_t is a function of the number of steps N_{step} and the step length L_{step} (4). The first is derived from the pedometer and detailed in Section IV-A1 while we elaborate on the step length in Section IV-A2.

$$d_t = N_{step} \cdot L_{step} \tag{4}$$

1) Pedometer insights and limits: In smartphones, the pedometer is computed by the firmware using the IMUs, making phones behave differently from one manufacturer to another. To evaluate this, the pedometer measurements from four different phones are superimposed in Figure 10. While almost all phones behave similarly, the Xiaomi 11T returns a value very infrequently, making it unusable. Additionally, when the user starts moving, the firmware lacks responsiveness to update the pedometer value. This behavior ranges from 5 s to 10 s as pointed in the Figure 11 and is documented by the manufacturer [20]. Unfortunately, this latency has a direct impact on our localization, with the first position being consistently very distant from the starting point.

2) Stride length estimation: The stride differs from one to another, and the distance covered depends on our pace, which varies over time. Therefore, predicting the distance covered in a single step is very challenging. Significant algorithmic proposals have been made to estimate this distance L_{step} [10], [11], and following the results from the deep learning

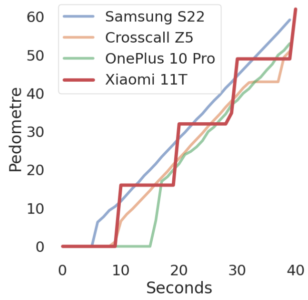

Fig. 10. Pedometer comparison between smartphones.

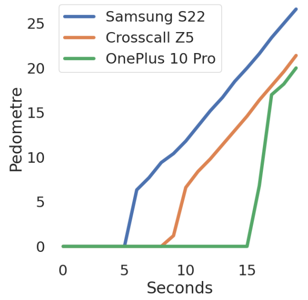

Fig. 11. Time between movement and first pedometer report.

study conducted by Hannink et al. [12], we have fixed this distance to 80 cm. Having a fixed rather than dynamic stride length have little impact on our results presented in Section IV-D, which prove consistent with previous work.

B. Heading detection

The direction is either based on a relative measurement by the accelerometer, or on an absolute measurement by the magnetometer. The latter, favored by previous propositions, relies on the Earth's magnetic field and can be affected by the presence of steel buildings, magnets, or various tools and devices. Extensive experiments conducted by Rai et al. [13] revealed an error of 15 degrees for 90% of the building surfaces. This result is in line with our observations in Section IV-D and can be used to estimate the overall error. On the other hand, the accelerometer produces a relative direction from a starting position and may be used to improve the magnetometer precision [9]. This system also requires knowing the orientation of the phone in space beforehand (vertical, horizontal, facing forward, or backward) using the built-in gyroscope. Additionally, calibrating the magnetometer and accelerometer can enhance the overall performance.

C. Measurement retrieval

In the Android architecture, the pedometer and the entire IMUs are exposed to Android APIs by the firmware. An application has been developed to collect all relevant data inside a CSV file. It was then deployed on different smartphones for comparisons in Sections IV-A and IV-D. Ideally, this measurement could be requested through LPP, but no UE currently implement this protocol. This passive recording will be replaced with a secured WebSocket connection to the LMF, thus centralizing data collection in the CN.

D. Experimentation

The PDR is evaluated on a track designed to represent typical human movements indoors, as depicted in Figure 12. The total distance and change of direction allow pedometer and magnetometer performance to be evaluated on four different smartphones. As this system has no knowledge on the actual position, all measurements share the same starting point at coordinates (0,0). The conclusions drawn from these experiments are detailed in Sections IV-D1 to IV-D4.

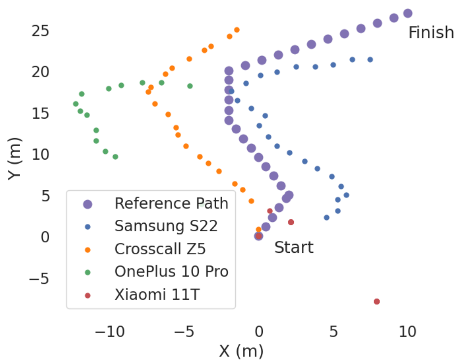

Fig. 12. PDR comparison between smartphones.

1) Global performance: The overall estimated shape and trajectory is quite faithful to the reference trace, demonstrating PDR reliability. More precisely, the estimated distance is close to the actual route taken by the user. The orientation is also consistent for all devices, underling the efficiency and reliability of the magnetometer regardless of the brand. However, a spatial shift can be observed, notably in the trajectory of the OnePlus, far from the truth. A few explanations for this behavior and some crucial points are therefore discussed next.

2) Offset between movement and first measurement: Because of the delay between the start of walking and the activation of the pedometer, the importance of the first estimated location is multiplied tenfold and tends to induce a position far from the truth. The OnePlus is the epitome of such of case, as the first point, delayed by more than 10 seconds according to Figure 11, is so out of sync that the overall shape is shifted by 10 meters. This delay can be corrected by implementing a more sensitive pedometer solution. However, this sensitivity leads to false positives, making it challenging to find a balance between reliability and speed.

3) Phone impact: Here, we confirm what was discussed in Section IV-A, noting that the Xiaomi and OnePlus, are poorly localized, for reasons explained earlier. The difference between the other phones is noticeable, but this variation depends heavily on the conditions of repetition, which are not perfect. Ten repetitions, performed in the next part and described in Section V-C, underline how reproducible the PDR is.

4) Intraspecific limitations and perspectives: By design, the PDR accumulates errors over time and cannot correct them. Here, all traces share the same origin, but if the user keeps walking, the new starting point will introduce very large errors into the subsequent trajectory. As highlighted by our work and many studies [9]–[13], frequent calibration is mandatory to make the most of this solution. Furthermore, calibration is mandatory as it links PDR to absolute coordinates. While some solutions involving RFID tags [21] have been suggested, we propose in the following a more scalable and global solution by leveraging existing wireless network.

V. PRILUN : A Fusion Between fingerprinting and PDR

Our experience with the use of fingerprinting and PDR has underlined how the former offers good overall performance and the latter good motion prediction. However, in fingerprinting, time is required to average the RSRP, making predictions imprecise during movement. PDR on the other hand, requires a known base position and regular calibration. Consequently, if the user is in motion, the PDR can be used with a starting point previously defined by fingerprinting. PDR calibration using fingerprinting can then be performed whenever the user stops. The fusion of these two methods is subsequently essential to obtain the best of both.

A. PRILUN

Few fusion algorithms have been proposed by previous works, some advocating weighting based on the presence of LOS [22], others suggesting shifting the trajectory based on fingerprinting [23], and still others adding Map Matching [24], [25]. All consider that RSRP based fingerprinting provides a minimally usable measure while the user is moving.

Contrary to the literature, we start from our experimental observation, detailed in Section V-B, that fingerprinting is not reliable enough when the user is in motion. Our algorithm called PDR and RSRP Interplay for Localization Using 5G Networks (PRILUN) and presented in Algorithm 1, is therefore different from the key works in the literature [22]–[25]. In PRILUN the intelligence is focused on user movement detection with a switch occurring between PDR if the user is moving and fingerprinting if the user is stationary. Our system therefore naturally compensates for PDR drift by calibrating its starting point using fingerprinting. The initial point is also set by fingerprinting, thus requiring no intervention whatsoever from the user. PRILUN was implemented and deployed in our 5G network, allowing us to evaluate it relative to fingerprinting and PDR alone.

Algorithm 1 PRILUN Pseudo-code

Require: UE_id
  while $LocalizationInProgress$ **do**
    $RSRP \leftarrow NRPPaMeasurements(UE\_id)$
    $Pos\_FP \leftarrow ML\_Predict(RSRP)$
    $Pedometer, Mag \leftarrow WebSocketMeas(UE\_id)$
    $(d, \theta) \leftarrow PDRTransform(Pedometer, Mag)$
    if d is null **then** ▷ If the user is static
      $CurentPos \leftarrow Pos\_FP$
      ▷ Use the fingerprinting prediction
    else
      $PosPDR \leftarrow PDRPredict(d, \theta, PreviousPos)$
  ▷ Use the PDR prediction
      $CurentPos \leftarrow PosPDR$
    end if
    $Emmit(CurentPos)$
    $PreviousPos \leftarrow CurentPos$
  end while

B. Experiments on realistic 5G infrastructure

1) Experimental protocol: To assess the effectiveness of the presented algorithm, the 5G infrastructure detailed in Section II-C is used. A user is initially stationary at his/her desk at the location called "Start". The user then moves to the "Pause" point where he/she stops for some time to talk to a colleague. The journey then continues to the break room for a coffee at the "Finish" point as shown in Figure 13.

During this time, the user is equipped with a 5G smartphone in his/her pocket, collecting PDR and RSRP measurements from our infrastructure. The two methods and their fusion are computed simultaneously, and results are presented in Figure 14 to 16.

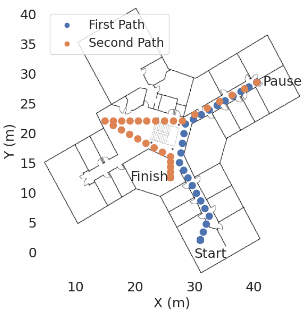

Fig. 13. Reference path.

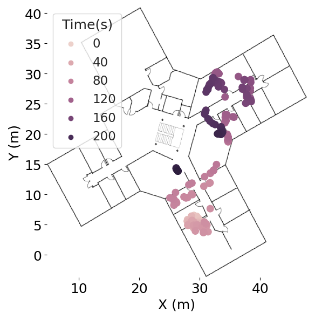

Fig. 14. ECID position prediction.

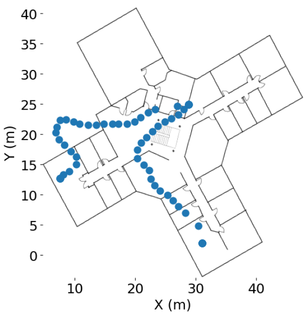

Fig. 15. PDR position prediction.

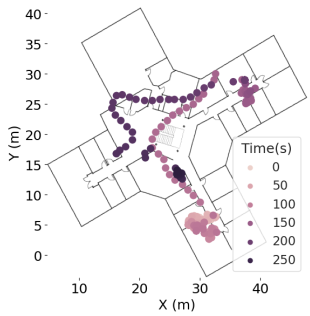

Fig. 16. PRILUN position prediction.

2) Fingerprinting and PDR performance: The experiments presented in Figure 14 highlight the fingerprinting performance. While the precision during static phases aligns with our observations in Section III-C, the accuracy degrades significantly when the user is in motion to the point where tracking becomes nearly impossible.

On the other hand, PDR exhibits the characteristics described in Section IV-D. The overall shape is satisfactory but shifted towards the south-west. Additionally, errors accumulate to the extent of estimating a position outside the building.

3) PRILUN performance: The major observation in Figure 16 is the drastic performance improvement by PRILUN. The overall shape is much more precise and get the most out of each method. It manages to calibrate the PDR during the "Pause" and even though the starting point from this position is not quite accurate, the system manages to produce a faithful trajectory estimation that is once more calibrated at "Finish". Moreover, a human can easily deduce the true path from the fusion alone.

4) Quantitative comparison: The error over time produced by fingerprinting and PDR is presented in Figure 17. When static, the mean error around $3\,\mathrm{m}$ is consistent with our results presented in Section III-C. During movements, the fingerprinting often reaches up to $20\,\mathrm{m}$ of error due to the rapidly changing radio context. It can also be noticed that the error produced by PDR is quite coherent with our previous experiments. At first, it manages to be in line with the real path, outperforming fingerprinting. But without calibration, its error increase over time until it no longer corresponds to a realistic position. It should also be noted that the initial error is zero, as we have manually set its initial point.

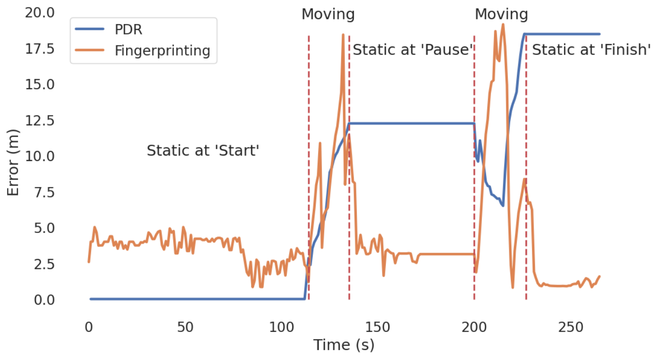

Fig. 17. The error produced over time by the PDR and ECID.

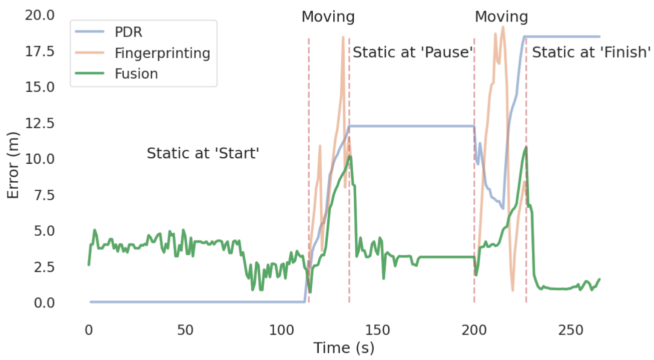

Fig. 18. The error produced over time by the fusion algorithm PRILUN.

The error produced by the fusion, shown in Figure 18, proves how PRILUN manages to always outperform the two methods taken separately. It strictly follows E-CID during static phases, and, thanks to PDR correction, it significantly reduces errors during movements. Thus, during the last move, the error is reduced by more than $10\,\mathrm{m}$ compared to PDR and fingerprinting alone. Overall, the average error is around $3\,\mathrm{m}$ to $4\,\mathrm{m}$, which is perfectly suitable for our needs to locate a worker in a risky situation.

C. About repeatability

To assess the accuracy of our results, we repeated the operation ten times, as shown in Figure 19. Notably, there is a significant consistency in results across all iterations. Both the “Start” and “Pause” points have good repeatability, with the “Pause” point in LOS performing best. The error produced during the movement is also consistent across all ten repetitions.

The only standout is the “Finish” point, which presents a unique challenge, as this room is located at the intersection of two cells, both at the limit of their range. A mere passage of an individual can lead to a loss of connection with one of the cells. In such cases, the algorithm estimates the position in an entirely different location, resulting in a substantial precision error. However, it should be noted that only a handful of cases behave in this way and that most repetitions provide a sufficient position to locate a worker in a dangerous situation. As these ambiguous locations represent the greatest challenge, they are labelled as such in our user map to better help the rescue team.

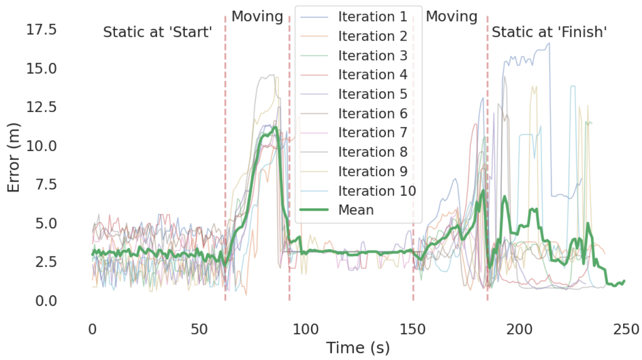

Fig. 19. Error produced by PRILUN during ten repetitions.

D. How to improve the initial point

The problem stated in Section IV-A about the lack of responsiveness between the start of movement and the first PDR notification by the firmware poses a substantial issue. Indeed, the first PDR point will be based on a RSRP measurement while the user is already in motion. This directly impacts the entire system and introduces an error that we can reduce. To address this, we propose not to base the first PDR position relative to the last E-CID position, but rather according to the average position over the entire duration the user was static.

The result presented in Figure 20 highlights the benefits of such an improvement, where the new version reduces the error during the second movement, as averaging the position during the “Pause” helps reduce the signal variance. However, during the first movement, the fingerprinting predicts a better position just before the movement, inducing no error reduction. Our experiments underline that this is only an occasional phenomenon, not representative of nominal system operation. In addition, setting a window on the order of a minute can reduce the error due to the movement of a person or an object between the UE and the radio.

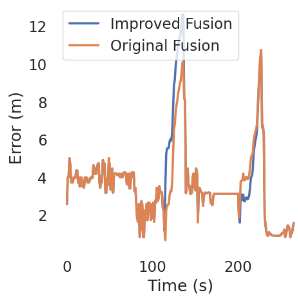

Fig. 20. Improved initial point for PRILUN.

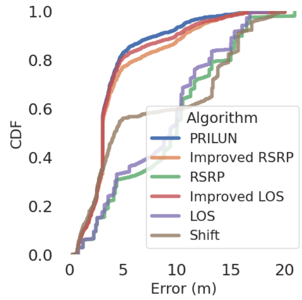

Fig. 21. Error Cumulative Distribution Function of multiple algorithms.

E. How does PRILUN compare with other algorithms

Now that PRILUN has been established to outperform ECID and PDR, it also must be compared to other similar algorithms. The first one is from the work of Cho and Kwon [22], which alternates between PDR and fingerprinting based on whether the UE is in LOS or not. The second algorithm is our design and arbitrates based on the received signal quality. If the signal is strong enough (with $RSRP > -80dB$), fingerprinting is used, otherwise the system switches to PDR prediction. The last algorithm from Chen et al. [23] uses fingerprinting predictions as reference points to shift the PDR predictions.

The ten-repetition presented in Section V-C were used as input data and the error Cumulative Distribution Function (CDF) are shown in Figure 21. The first algorithm is denoted “LOS”, the second “RSRP” and the third “Shift”. We also propose to improve the first two by adding a movement detection phase before applying these algorithms, ensuring that they only perform when the user is in motion. From the results, we can affirm that this improvement is vital and drastically improves precision. But even with the proposed improvements, the figure clearly shows that PRILUN manages to surpass the other algorithms. This can be explained by the others considering fingerprinting predictions valid during movement, contrary to PRILUN. Not only does it manage to outperform both fingerprinting and PDR, it also ranks first among fusion algorithms.

VI. Related work

This work is partly based on our previous study of E-CID and fingerprinting [4]. E-CID has already been explored by others in the context of 5G, with some studies having provided interesting experimental results [3], [4], [8]. An experimental 5G study called iPos [3] also employs fingerprinting but relies on Channel State Information (CSI) measurements. The common conclusion is that to improve fingerprinting accuracy, deployment density needs to be increased, which is challenging given the cost of a 5G network.

In the realm of PDR, the widespread availability of IMUs in smartphones has led to a surge in interest. Numerous solutions have been proposed, as documented in surveys [9] and algorithmic comparisons [10]. The main challenges in PDR today include estimating stride length, for which an elegant solution has been proposed by Krieg et al. [11]. Advanced studies in Deep Learning, such as the one by Hannink et al. [12], show promising results for end-to-end system integration. Finally, reducing the overall error can be achieved by using both accelerometer and magnetometer [13] or RFID tags [21].

To the best of our knowledge, our work is pioneering, and there are no known research studies specifically addressing the fusion of RSRP and PDR in the context of 5G. However, several studies have focused on Received Signal Strength (RSS) measurements in Wi-Fi environments with some approaches combining PDR, RSS, and Map Matching [24], [25]. The comprehensive work of Zampella et al. [24] achieves impressive results approximately $1\,\mathrm{m}$ accuracy, although its complexity and resource requirements are significant when compared to the Maximum Likelihood solution proposed by Chen et al. [23]. The latter suggests shifting the PDR path according to fingerprinting measurements, which therefore serves as a reference for global direction. All these studies assume RSS measurements are always valid and employ weighting strategies between PDR and fingerprinting. This differs from that of Cho and Kwon [22], who consider RSS valid only in LOS scenarios and switch to PDR in NLOS conditions.

VII. Conclusion

This paper lays the groundwork for the most comprehensive and practical indoor localization solution in 5G, based on standard commercial equipment and taking advantage of existing networks. In this context, the only two viable methods, namely fingerprinting and the PDR, are implemented and deployed in our 5G infrastructure. The conclusions drawn from our experiments argue for a fusion of these two by our algorithm PRILUN, in which the weaknesses of one are offset by the strengths of the other. Through extensive experiments, we demonstrated how our solution outperformed PDR, fingerprinting, and other similar fusion algorithms. This comprehensive localization framework is a major asset for innovative networks aiming for digital frugality. Since our methodology considered all aspects of 5G, an improvement could be to leverage other radio networks, such as Wi-Fi or public cellular networks.

References

[1] Alsatis, "Network integrator in toulouse, france," 2023. [Online]. Available: https://alsatis.com/

[2] M. Gucciardo, I. Tinnirello, G. M. Dell'Aera, and M. Caretti, "A Flexible 4G/5G Control Platform for Fingerprint-based Indoor Localization," in *IEEE INFOCOM Workshops*, apr 2019, pp. 744–749.

[3] Y. Ruan, L. Chen, X. Zhou, Z. Liu, X. Liu, G. Guo, and R. Chen, "iPos-5G: Indoor Positioning via Commercial 5G NR CSI," *IEEE Internet of Things Journal*, vol. 10, no. 10, pp. 8718–8733, May 2023, conference Name: IEEE Internet of Things Journal.

[4] A. Le Floch, R. Kacimi, P. Druart, Y. Lefebvre, and A.-L. Beylot, "Accurate E-CID Framework for Indoor Positioning in 5G using Path Tracing and Machine Learning," in *Proceedings of the Int'l ACM Conference on Modeling Analysis and Simulation of Wireless and Mobile Systems*. Montreal Quebec Canada: ACM, Oct. 2023, pp. 9–17. [Online]. Available: https://dl.acm.org/doi/10.1145/3616388.3623406

[5] Firecell, "Precise indoor tracking with private 5g," 2023. [Online]. Available: https://firecell.io/fr/learn/geo5g/

[6] L. Taponecco, A. D'Amico, and U. Mengali, "Joint toa and aoa estimation for uwb localization applications," *IEEE Transactions on Wireless Communications*, vol. 10, no. 7, pp. 2207–2217, 2011.

[7] G. Deak, K. Curran, and J. Condell, "A survey of active and passive indoor localisation systems," *Computer Communications*, vol. 35, no. 16, pp. 1939–1954, Sep. 2012. [Online]. Available: https://linkinghub.elsevier.com/retrieve/pii/S014036641200196X

[8] D. Li, X. Chu, L. Wang, Z. Lu, S. Zhou, and X. Wen, "Performance Evaluation of E-CID based Positioning on OAI 5G-NR Testbed," in *2022 IEEE/CIC International Conference on Communications in China (ICCC)*, Aug. 2022, pp. 832–837, iSSN: 2377-8644.

[9] R. Harle, "A Survey of Indoor Inertial Positioning Systems for Pedestrians," *IEEE Communications Surveys & Tutorials*, vol. 15, no. 3, pp. 1281–1293, 2013, conference Name: IEEE Communications Surveys & Tutorials.

[10] A. Jimenez, F. Seco, C. Prieto, and J. Guevara, "A comparison of Pedestrian Dead-Reckoning algorithms using a low-cost MEMS IMU," in *2009 IEEE International Symposium on Intelligent Signal Processing*, Aug. 2009, pp. 37–42.

[11] J.-G. Krieg, G. Jakllari, H. Toma, and A.-L. Beylot, "Acrux: Indoor Localization Without Strings," in *Proceedings of the 20th ACM International Conference on Modelling, Analysis and Simulation of Wireless and Mobile Systems*. Miami Florida USA: ACM, Nov. 2017, pp. 187–196. [Online]. Available: https://dl.acm.org/doi/10.1145/3127540.3127545

[12] J. Hannink, T. Kautz, C. F. Pasluosta, J. Barth, S. Schülein, K.-G. Gaßmann, J. Klucken, and B. M. Eskofier, "Mobile stride length estimation with deep convolutional neural networks," *IEEE journal of biomedical and health informatics*, vol. 22, no. 2, pp. 354–362, 2017.

[13] A. Rai, K. K. Chintalapudi, V. N. Padmanabhan, and R. Sen, "Zee: zero-effort crowdsourcing for indoor localization," in *Proceedings of the 18th annual international conference on Mobile computing and networking*. Istanbul Turkey: ACM, Aug. 2012, pp. 293–304. [Online]. Available: https://dl.acm.org/doi/10.1145/2348543.2348580

[14] 3GPP, "5g system; location management services; stage 3 (3gpp ts 29.572 version 18.1.0 release 18)," Third-generation Partnership Project (3GPP), Standard, Mar. 2023.

[15] Amarisoft, "Test and field 5g equipment," 2023. [Online]. Available: https://www.amarisoft.com/

[16] Halys, "Halys 5g core network," 2023. [Online]. Available: https://www.halys.fr/

[17] AW2S, "5g radio," 2023. [Online]. Available: https://www.aw2s.com/fr/

[18] Crosscall, "5g smartphones," 2023. [Online]. Available: https://www.crosscall.com/

[19] F. Pedregosa, G. Varoquaux, A. Gramfort, V. Michel, B. Thirion, O. Grisel, M. Blondel, P. Prettenhofer, R. Weiss, V. Dubourg, J. Vanderplas, A. Passos, D. Cournapeau, M. Brucher, M. Perrot, and E. Duchesnay, "Scikit-learn: Machine learning in Python," *Journal of Machine Learning Research*, vol. 12, pp. 2825–2830, 2011.

[20] "Samsung health step," https://developer.samsung.com/health/android/data/api-reference/com/samsung/android/sdk/healthdata/HealthConstants.StepCount.html, accessed: 2023-12-04.

[21] S. House, S. Connell, I. Milligan, D. Austin, T. L. Hayes, and P. Chiang, "Indoor localization using pedestrian dead reckoning updated with rfid-based fiducials," in *2011 Annual International Conference of the IEEE Engineering in Medicine and Biology Society*, 2011, pp. 7598–7601.

[22] H. Cho and Y. Kwon, "RSS-based indoor localization with PDR location tracking for wireless sensor networks," *AEU - International Journal of Electronics and Communications*, vol. 70, no. 3, pp. 250–256, 2016. [Online]. Available: https://www.sciencedirect.com/science/article/pii/S1434841115003398

[23] L.-H. Chen, E. H.-K. Wu, M.-H. Jin, and G.-H. Chen, "Intelligent Fusion of Wi-Fi and Inertial Sensor-Based Positioning Systems for Indoor Pedestrian Navigation," *IEEE Sensors Journal*, vol. 14, no. 11, pp. 4034–4042, Nov. 2014, conference Name: IEEE Sensors Journal.

[24] F. Zampella, A. R. Jimenez Ruiz, and F. Seco Granja, "Indoor Positioning Using Efficient Map Matching, RSS Measurements, and an Improved Motion Model," *IEEE Transactions on Vehicular Technology*, vol. 64, no. 4, pp. 1304–1317, Apr. 2015. [Online]. Available: http://ieeexplore.ieee.org/document/7008540/

[25] L.-F. Shi, Y. Wang, G.-x. Liu, S. Chen, Y.-L. Zhao, and Y.-F. Shi, "A Fusion Algorithm of Indoor Positioning Based on PDR and RSS Fingerprint," *IEEE Sensors Journal*, vol. 18, no. 23, pp. 9691–9698, Dec. 2018, conference Name: IEEE Sensors Journal.